Supporting Information

Bioinspired Silica-Shell Coacervates: Enhanced Stability and Functional Versatility

Yitong Wang[1], *Yixin Yun*[1], *Janar Tursen*[1], *Yuang Tang*[1], *Hongke Zhang*[1], *Xiaoqi Song*[1], *Xiaona Yu*[4], *Lujia Han*[3], *Wanbin Zhu*[1,2], *Hongliang Wang*[1,2*]

[1]Center of Biomass Engineering/College of Agronomy and Biotechnology, China Agricultural University, Beijing 100193, P.R. China

[2]Sanya Institute of China Agricultural University, Sanya 572025, P.R. China

[3]Engineering Laboratory for AgroBiomass Recycling & Valorizing, College of Engineering, China Agricultural University, Beijing 100083, P.R. China

[4]College of Resources and Environment, Henan Agricultural University, Zhengzhou 450046, P.R. China

*Hongliang Wang

E-mail: hlwang@cau.edu.cn

Includes:

Supplementary figures, Fig.S1 to Fig.S21

Supplementary tables, Table.S1 to Table.S2

Supplementary figures

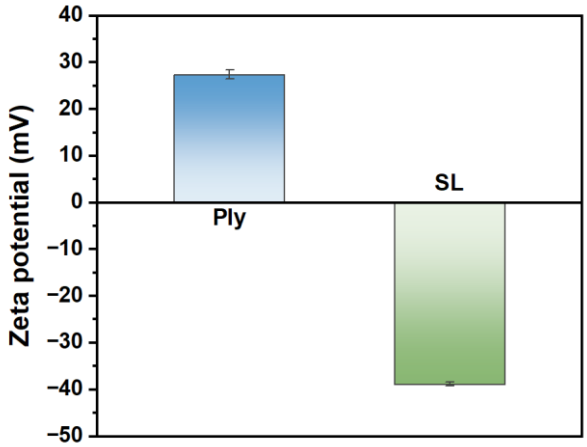

Fig.S1 Zeta potential of Ply and SL in aqueous solution.

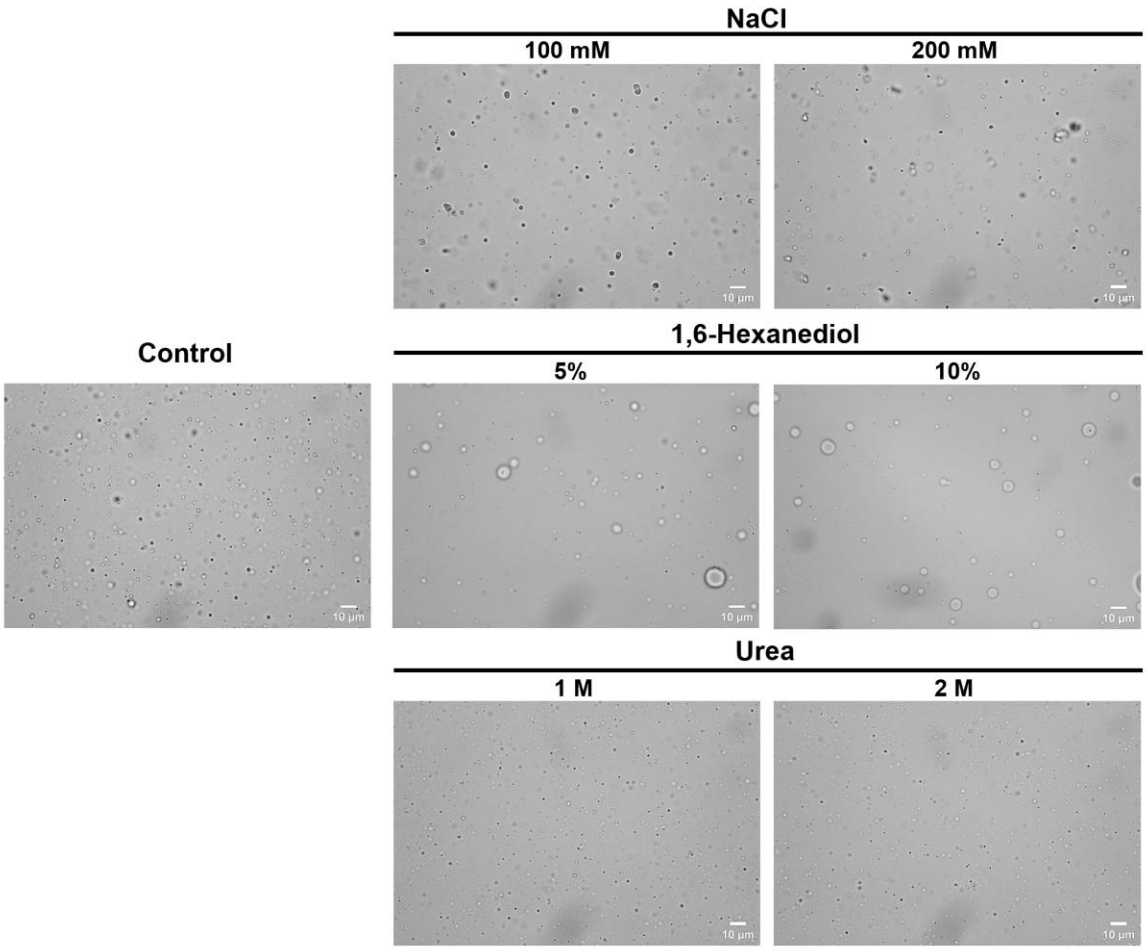

Fig.S2 Effects of NaCl (electrostatic interaction disruptor), 1,6-hexanediol (hydrophobic interaction disruptor), and urea (hydrogen bond disruptor) on coacervates formation.

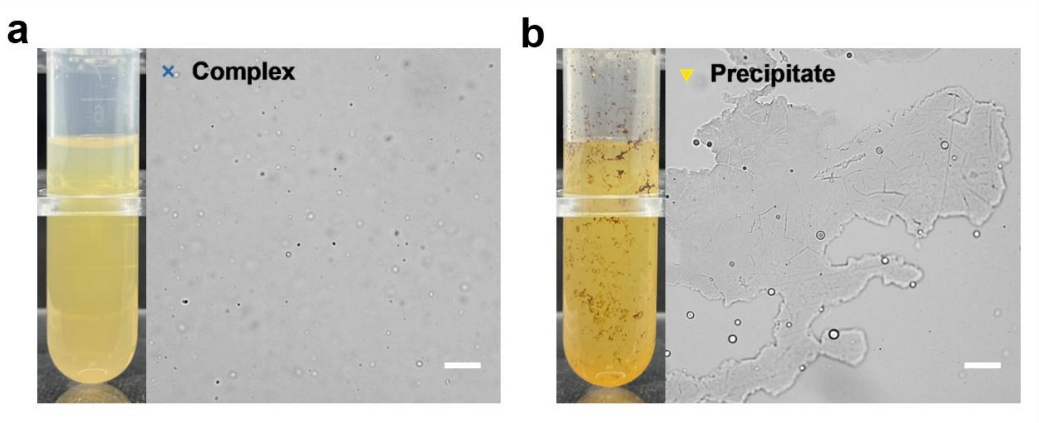

Fig.S3 Macroscopic and microscopic images (scale bar = 10 μm) of soluble complex (**a**) and solid precipitate (**b**). The conditions of (a) were pH 7, c_{SL}=1 g L^{-1}, c_{Ply}=1 g L^{-1}. The conditions of (b) were pH 7, c_{SL}=3 g L^{-1}, c_{Ply}=1 g L^{-1}.

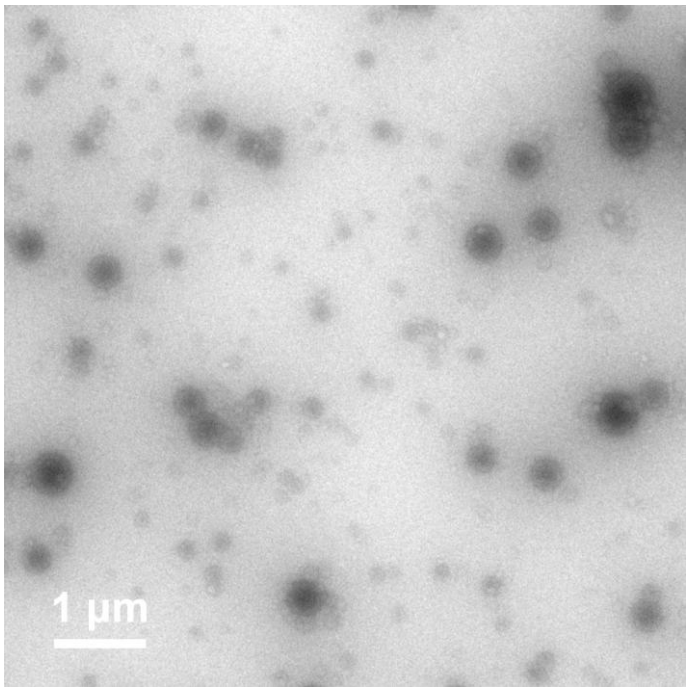

Fig.S4 TEM image of SL/Ply/$Si_{1.2\%}$ after aging for 24 h at low magnification.

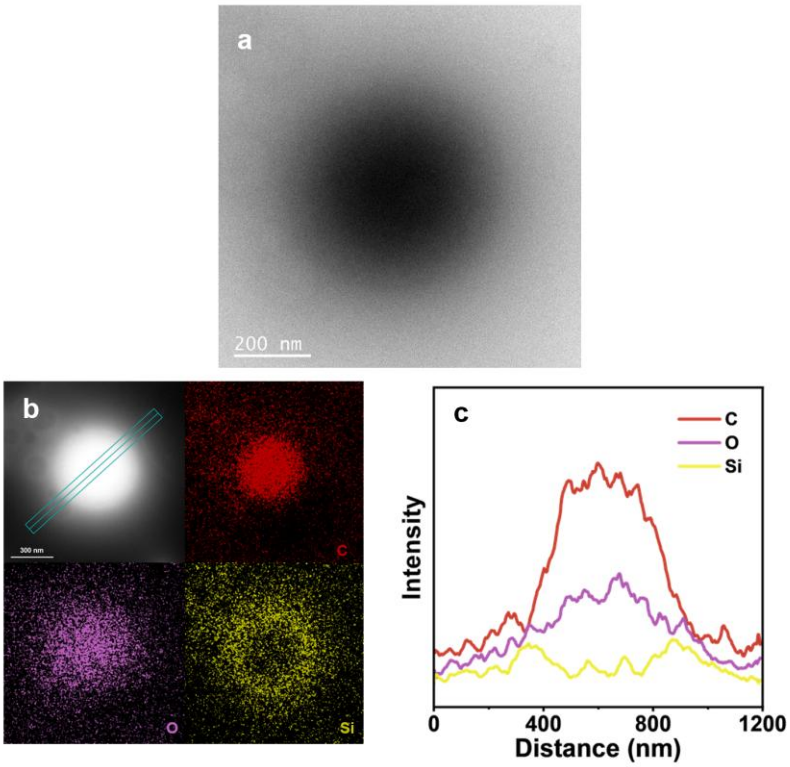

Fig.S5 a) TEM image, **b**) TEM-EDX elemental mapping image and **c**) corresponding line scanning image of SL/Ply/$Si_{0.4\%}$ after aging for 24 h.

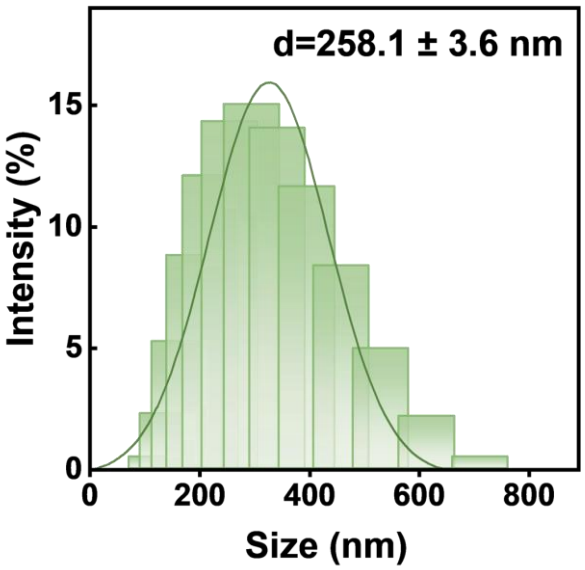

Fig.S6 Size distribution of SL/Ply/$Si_{0.8\%}$ after aging for 24 h.

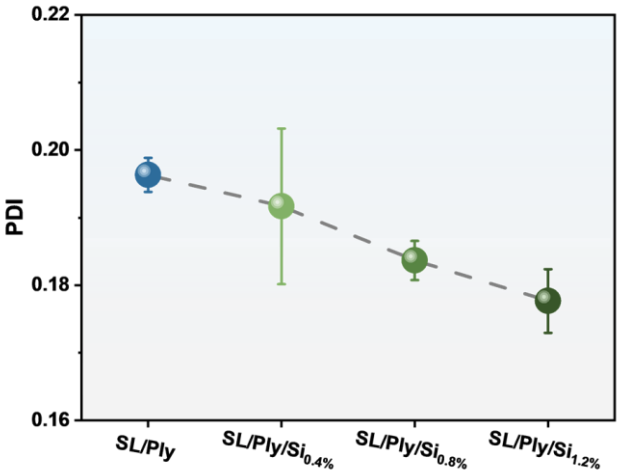

Fig.S7 PDI values of SL/Ply and SL/Ply/Si$_n$ coacervates.

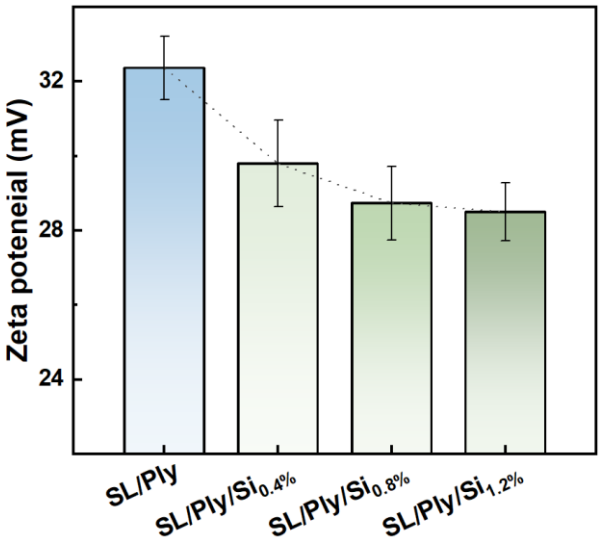

Fig.S8 Zeta potential of SL/Ply and SL/Ply/Si$_n$ coacervates.

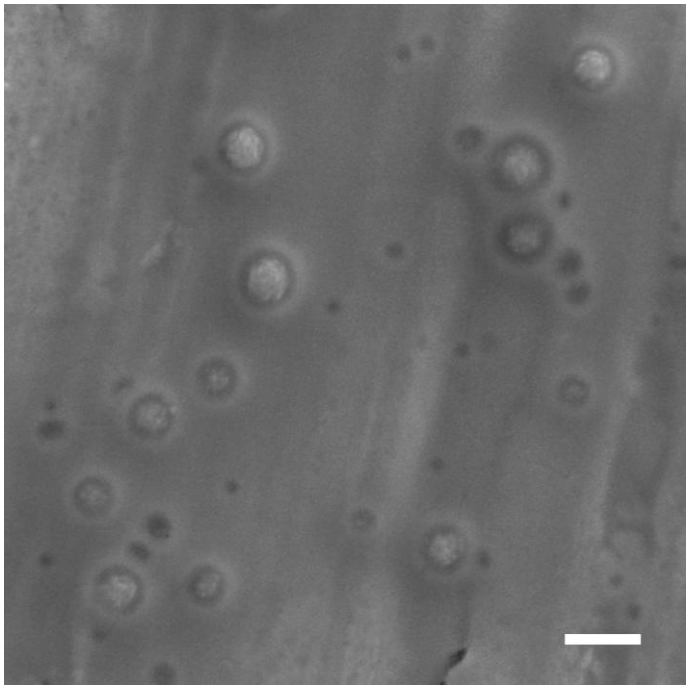

Fig.S9 SEM image of the macroscopic liquid phase of SL/Ply/$Si_{5.0\%}$. Scale bar = 400 nm.

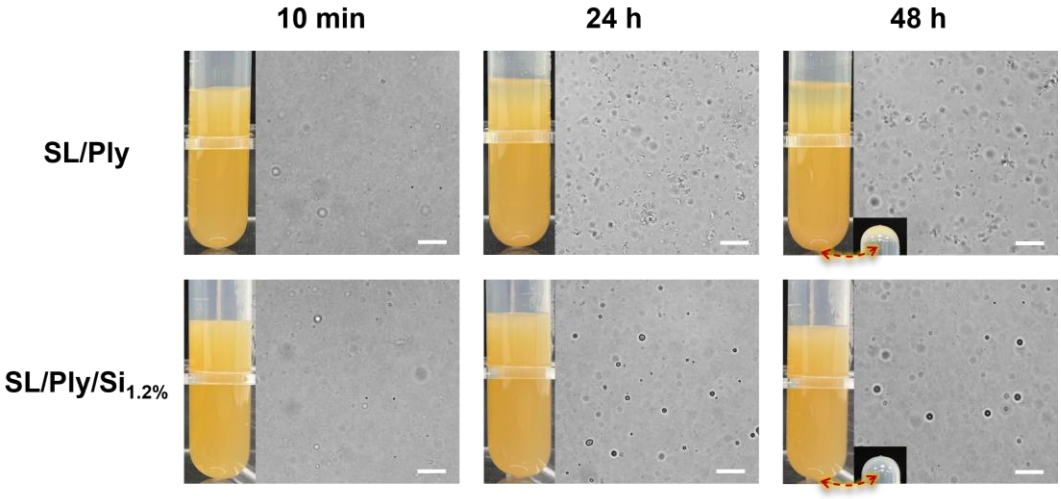

Fig.S10 Macroscopic and microscopic images (scale bar = 10 μm) of SL/Ply and SL/Ply/$Si_{1.2\%}$ after different storage durations.

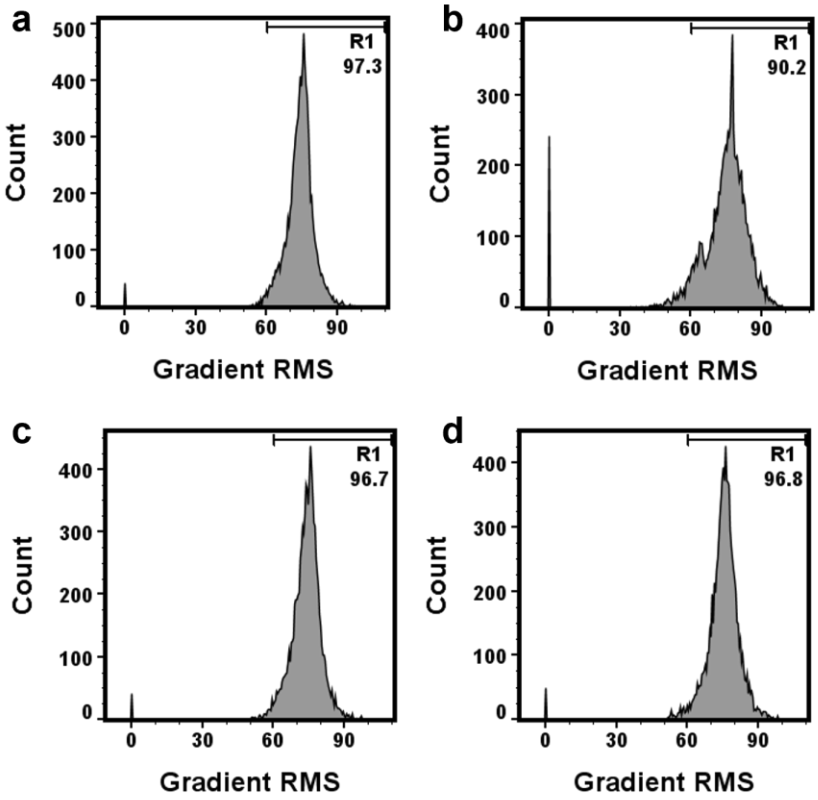

Fig.S11 Gating strategy based on Gradient RMS in IFC defining the well-focused population R1. **a**) SL/Ply at 1 h, **b**) SL/Ply at 48 h, **c**) SL/Ply/$Si_{1.2\%}$ at 1 h, **d**) SL/Ply/$Si_{1.2\%}$ at 48 h.

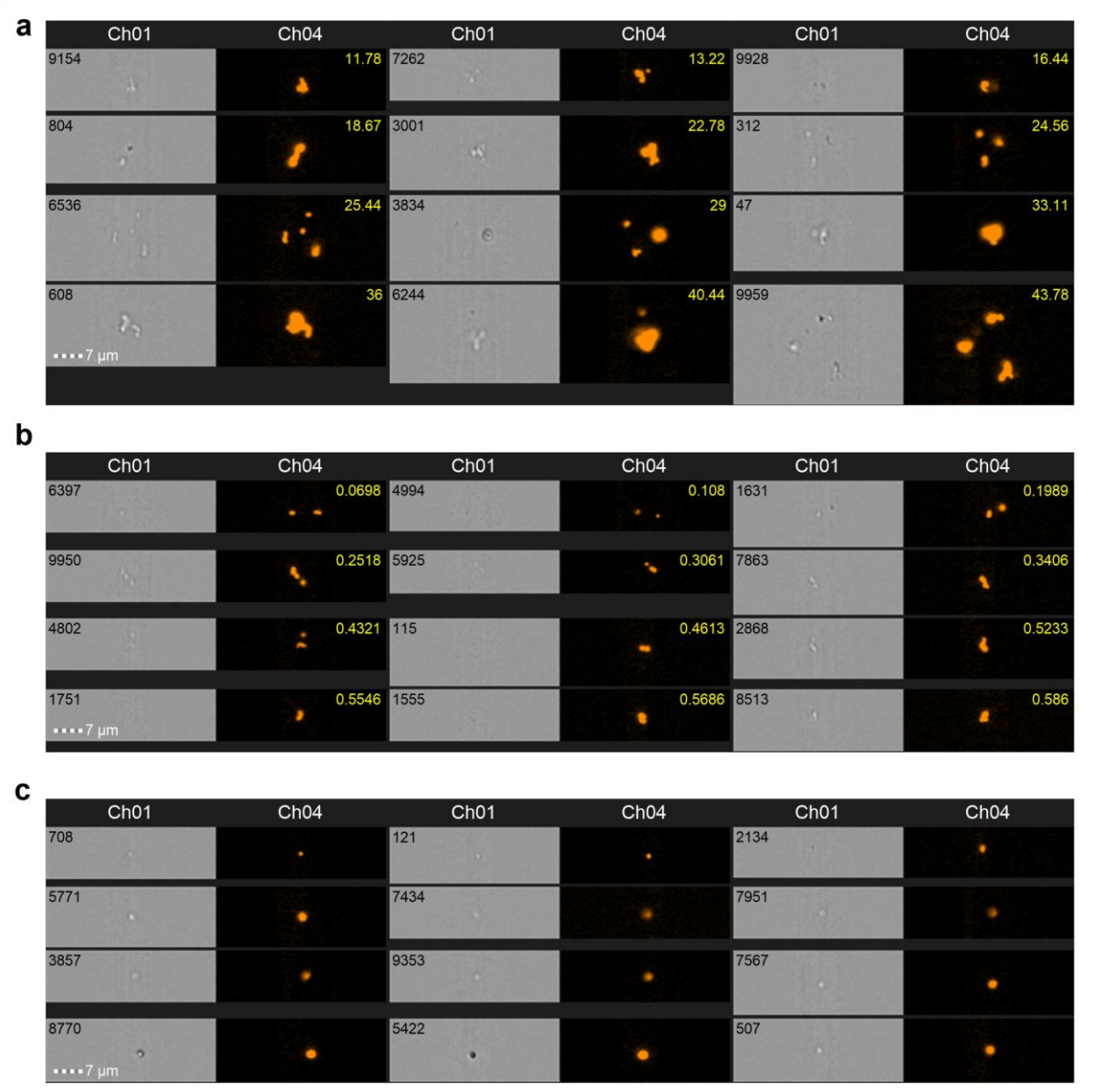

Fig.S12. Representative images: **a**) Oversize events excluded from analysis; the yellow number in the upper right corner indicates the area values. **b**) Low-aspect-ratio-intensity events excluded from analysis; the yellow number in the upper right corner indicates the aspect ratio intensity values. **c**) R2 population. Ch01: Bright field; Ch04: Fluorescence (Rhodamine 6G). The event ID was displayed in the upper left corner of the bright field images. All images from SL/Ply at 1 h post-preparation.

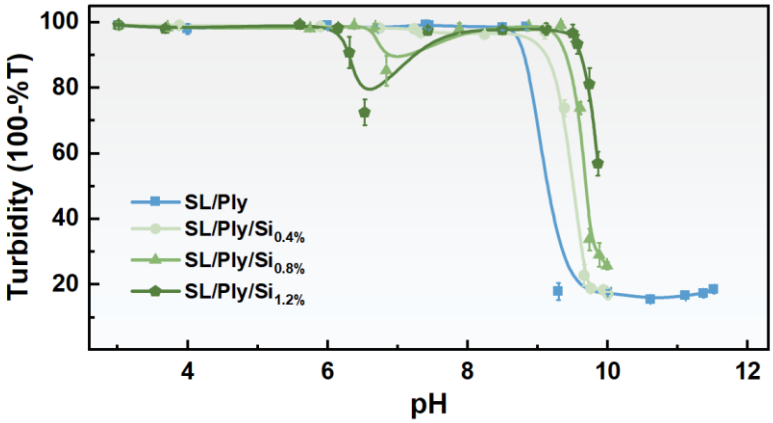

Fig.S13 The effect of different pH values on the turbidity of the SL/Ply and SL/Ply/Si_n coacervates.

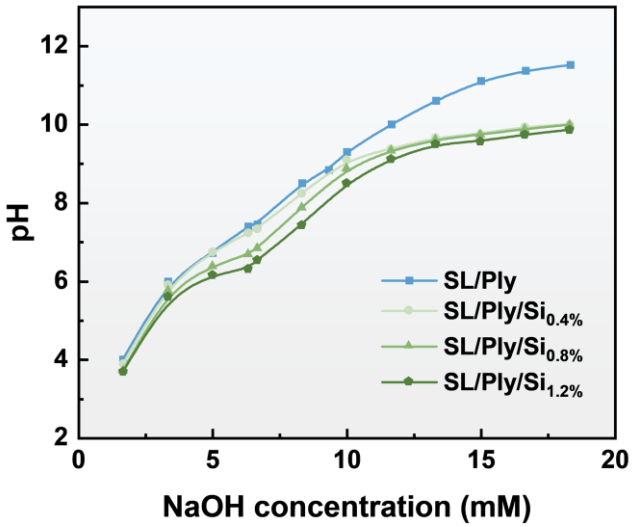

Fig.S14 Influence of NaOH concentration on the pH of SL/Ply and SL/Ply/Si_n coacervates.

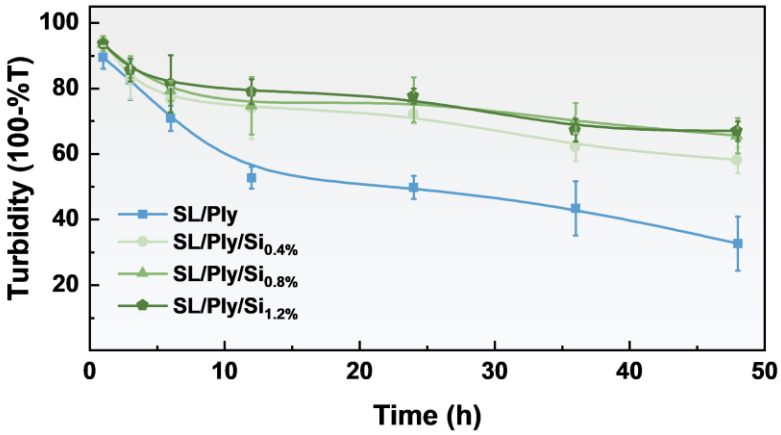

Fig.S15 The effect of mechanical shaking time on the turbidity of the SL/Ply and SL/Ply/Si$_n$ coacervates.

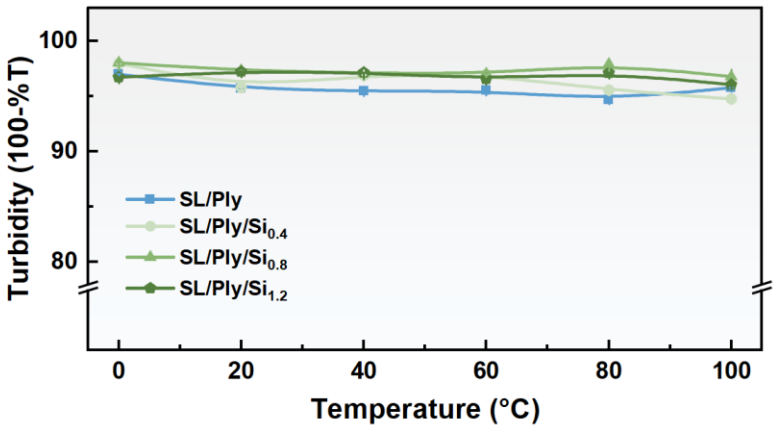

Fig.S16 The effect of different temperatures on the turbidity of the SL/Ply and SL/Ply/Si$_n$ coacervates.

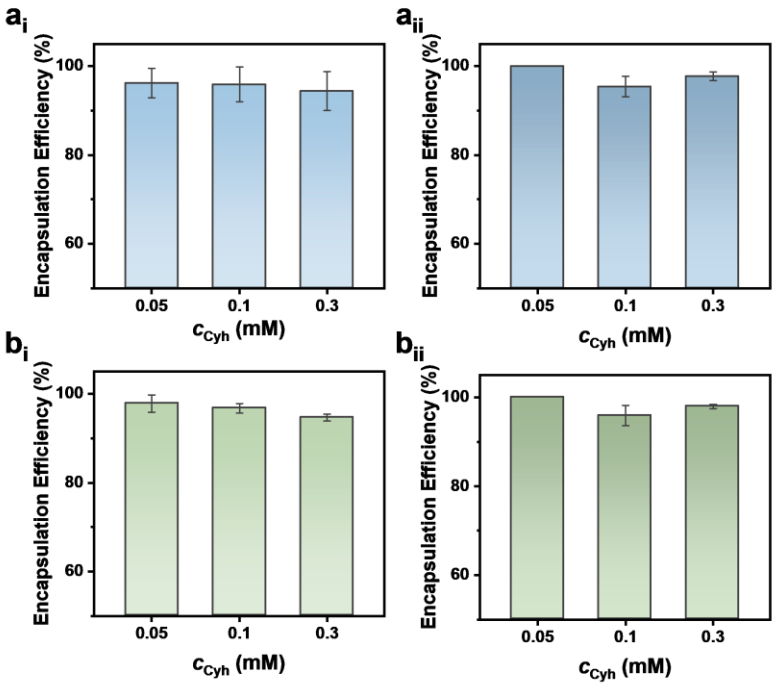

Fig.S17 Encapsulation efficiency of Cyh@SL/Ply (**a**) and Cyh@SL/Ply/$Si_{1.2\%}$ (**b**) at day 1 (**a_i**, **b_i**) and day 5 (**a_{ii}**, **b_{ii}**).

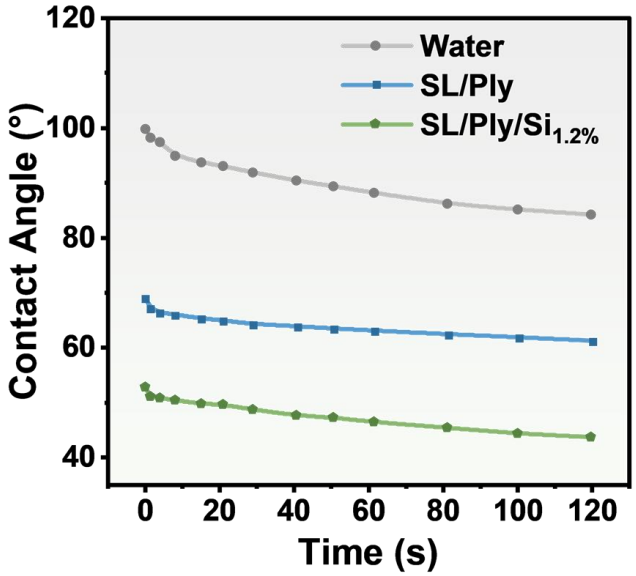

Fig.S18 Dynamic contact angle curves of water, SL/Ply and SL/Ply/$Si_{1.2\%}$ on Chinese cabbage leaves.

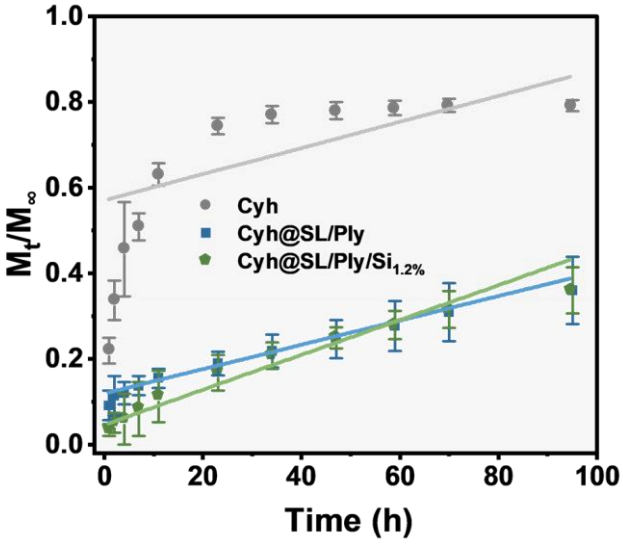

Fig.S19 Zero-order kinetic fitting curves for the release of technical Cyh, Cyh@SL/Ply, and Cyh@SL/Ply/$Si_{1.2\%}$.

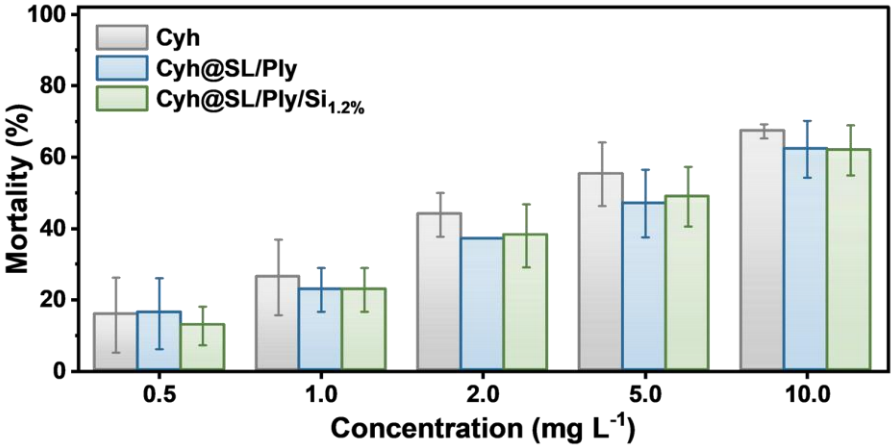

Fig.S20 Insecticidal activity of technical Cyh, Cyh@SL/Ply, and Cyh@SL/Ply/$Si_{1.2\%}$ at different concentrations against 3rd instar larvae of *P. xylostella* at 36 h.

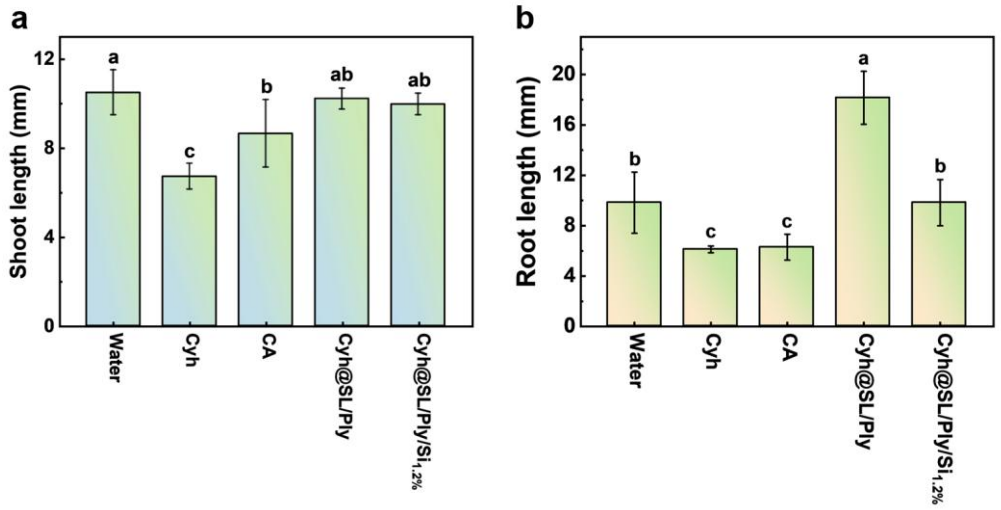

Fig.S21 Shoot length (**a**) and root length (**b**) of Chinese cabbage seeds under different treatments.

Supplementary tables

Table.S1 Fitting results for different release kinetic models.

Kinetic model	Samples	Fitted equation	R^2
Zero-order	Cyh	y=0.0031x+0.5677	0.3899
	Cyh@SL/Ply	y=0.0029x+0.1145	0.9616
	Cyh@SL/Ply/$Si_{1.2\%}$	y=0.0041x+0.0410	0.9666
First-order	Cyh	$y=0.7819(1-e^{-0.1690t})$	0.9503
	Cyh@SL/Ply	$y=0.2342(1-e^{-0.1288t})$	0.5353
	Cyh@SL/Ply/$Si_{1.2\%}$	$y=0.3467(1-e^{-0.0295t})$	0.9563
Ritger-Peppas	Cyh	$y=0.3878t^{0.1708}$	0.8043
	Cyh@SL/Ply	$y=0.0757t^{0.3116}$	0.9565
	Cyh@SL/Ply/$Si_{1.2\%}$	$y=0.0329t^{0.5262}$	0.9990

Table.S2 Median lethal concentration (LC_{50}) values of technical Cyh, Cyh@SL/Ply, and Cyh@SL/Ply/$Si_{1.2\%}$ against 3rd instar larvae of *P. xylostella* at 36 h and 48 h.

Time (h)	Samples	LC_{50} (mg/L)	95% Confidence interval	Fitted equation
36	Cyh	3.086	1.895–5.934	y = 1.014x−0.496
	Cyh@SL/Ply	4.302	2.497–11.669	y = 0.905x−0.573
	Cyh@SL/Ply/$Si_{1.2\%}$	4.262	2.545–10.504	y = 0.963x−0.606
48	Cyh	2	1.150–3.385	y = 1.014x−0.305
	Cyh@SL/Ply	1.416	0.741–2.277	y = 1.048x−0.158
	Cyh@SL/Ply/$Si_{1.2\%}$	1.187	0.659–1.793	y = 1.227x−0.091